EPJ manuscript No.
(will be inserted by the editor)

Nonlinear soliton-like excitations in twodimensional lattices and charge transport

A. P. Chetverikov[1,2], W. Ebeling[2,3], and M. G. Velarde[2,4]

[1] Dept. of Physics, Saratov State University, Astrakhanskaya 83, Saratov-410012, Russia
e-mail: chetverikovap@info.sgu.ru
[2] Instituto Pluridisciplinar, Universidad Complutense,
Paseo Juan XXIII, 1, Madrid-28040, Spain
e-mail: mgvelarde@pluri.ucm.es
[3] Institut für Physik, Humboldt-Universität Berlin, Newtonstrasse 15, Berlin-12489, Germany
e-mail: ebeling@physik.hu-berlin.de
[4] Fundacion Universidad Alfonso X El Sabio, Villanueva de la Canada, Madrid-28691, Spain

Abstract. We study soliton-like excitations in several two-dimensional lattices: square lattices including ones with externally fixed square lattice frame (cuprate model), and triangular lattices. We offer computational evidence of the possibility of fast lattice solitons and corresponding supersonic nearly loss-free transport of electrons bound to lattice solitons along crystallographic axes.

1 Introduction

Applications of nonlinear dynamics are a field of growing interest [1]. Of special interest are collective phenomena in two-dimensional lattices, which are so far only partially explored [2]. In the present work we study soliton-like collective excitations in two-dimensional systems of particles with strongly nonlinear interactions. In principle this is a quite old topic of natural sciences from hydraulics to optics, Bose-Einstein condensates etc.. Important work on the theory of two-dimensional solitons is due to Kadomtsev, Petiashvili, Zakharov and collaborators [3–5], see also [6–18]. More recently acoustic solitons on piezoelectric solid substances attracted interest [19, 20], in particular applications to the control and transport of charges [21,22,20,23–26]. Further we mention the observations of localized excitations (localized breathers, quodons) in layered structures like muscovite mica [30,31] and finally the excitations in cuprate layers [31,32,34,35].

We further discuss the problem of control of electrons by acoustic lattice soliton excitations, a form of electron *surfing*, which may have different origin such as e.g. mechanical or electrical shocks generated by contacts of the tip of an electron field microscope with a suitable anharmonic crystal lattice layer. We consider systems of a few hundred atoms on a plane interacting with one or a few added, excess electrons, earlier we have already discussed the interaction between electrons and strongly localized lattice excitations of soliton-type in one- (1d) and two-dimensional (2d) lattices [25,26]. For the electron dynamics we used the tight-binding approximation (TBA) and for the lattice particles a classical Hamiltonian with Morse interactions. As a result of this mixed classical-quantum dynamics we could show that the electrons "like" to follow the trajectories of the lattice soliton-like excitations. In the 1d case we have predicted several interesting phenomena, in particular the "vacuum-cleaner" effect, i.e., the electron probability density is gathered by solitons which along their trajectory act as long range attractors [36–38]. Noteworthy is that these excitations move in general with *supersonic* velocity, v_s, or velocities a bit below the sound velocity depending on the parameter values,

on the initial conditions and on the electron-lattice interaction [37]. This means that electrons bound to lattice solitons (in short called solectrons) can move with quite high velocities.

In the last part we consider the *anharmonic* lattice with an added, excess electron with charge e hopping from site to site along the lattice. The electron interacts with the initially neutral lattice atoms, shifts their energy levels and locally induces electric polarization in neighboring lattice sites.

2 Excitations in square lattices

Square lattices in 2d are closely related to 1d lattices since they may be considered as just 2 perpendicular crossed 1d-lattices. Each atom has 4 nearest neighbors and we have 2 crystallographic axes. We expect therefore 2 quasi 1d excitations along the crystallographic axes. Depending on the forces, there might be problems with he stability of square lattices, and this we will discussed in the next section. Assuming the the atoms have the coordinates $\mathbf{r_k}$ and the

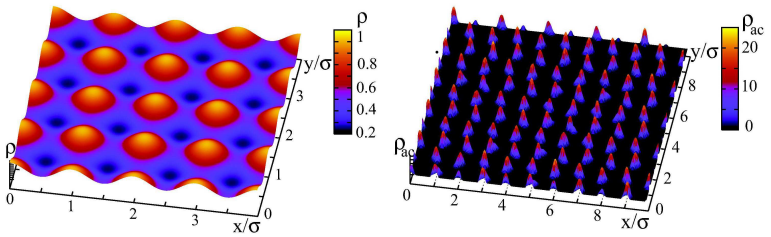

Fig. 1. Square lattice: The core densities of the lattice units/atoms. Left panel: Small part of an ideal square lattice. Right panel: Lattice consisting of $20 \cdot 20$ atoms including some displacements due to noise/temperature.

velocities $\mathbf{v_k}$ the Hamiltonian of our 2d system is

$$H = \frac{m}{2}\sum_k v_k^2 + \frac{1}{2}\sum_{k,j} V(r_k,\, r_j) \tag{1}$$

The subscripts locate the atoms all with equal mass, m, at lattice sites and the summations run from 1 to N. We shall assume that the lattice units repel each other with exponentially repulsive forces and attract each other with weak dispersion forces. The characteristic length determining the repulsion between the particles in the lattice is σ. We limit ourselves to nearest-neighbors only using the relative distance $r = |r_n - r_k|$. The above conditions are met by the Toda, V_T, and the Morse, V_M, potentials respectively:

$$V_T(r) = -D + \frac{M\omega_0^2}{b_T^2}(\exp(-b_T r') - 1 + b_T r'), \tag{2}$$

$$V_M(r) = -D\left\{2\exp[-br'] - \exp[-br']\right\}, \qquad r' = (r-\sigma), \qquad M\omega_0^2 = 2Db$$

To have dimensionless variables we consider the spatial coordinates rescaled with σ as unit length. Time is normalized to the inverse frequency of linear oscillations near the minimum of the potential well, ω_0^{-1}, whereas energy is scaled with twice the depth of the well $2D$. Further the stiffness parameters b and b_T (made dimensionless) define the strength of the repulsion between atoms. Note that with the choice $b_T = 3b$ the two potentials agree up to the third derivatives around the potential minimum. In the simulations we use a smooth cutoff of the potential at 1.5σ, excluding unphysical cumulative interaction effects arising from the influence of lattice units outside the first neighborhood of each atom [25]. To study, at varying temperature, the

nonlinear excitations of the lattice and the possible electron transport in a lattice in the simplest approximation it is sufficient to know the coordinates of the lattice (point) particles at each time and the interaction of lattice deformations with electrons. Coordinates and velocities of particles are obtained by solving the equations of motion of each particle under the influence of all possible forces. Our simulation algorithm corresponds to a molecular dynamics code, i.e. the particles are not fixed to any lattice node but may move freely through the system, exchanging places with neighbors etc.. Rather than using Cartesian coordinates x and y, we use complex coordinates $Z = x+iy$. Then the initial classical Newton deterministic equations corresponding to the lattice Hamiltonian (1) including also friction and random forces yields to a Langevin dynamics for the lattice units

$$\frac{d^2 Z_i}{dt^2} = \sum_k F_{ik}(Z_{ik}) z_{ik} + \left[-\gamma \frac{dZ_i}{dt} + \sqrt{2D_v}\,(\xi_{ix} + i\xi_{iy}) \right], \tag{3}$$

where again an index i identifies a particle among all N particles of the ensemble, γ is a friction coefficient, D_v defines the intensity of stochastic forces, $\xi_{ix,y}$ denotes statistically independent generators of the Gaussian noise. $T = mD_v/\gamma$ (Einstein's relation). $Z_{ik} = Z_i - Z_k$ and $z_{ik} = (Z_i - Z_k)/|Z_i - Z_k|$ is the unit vector defining the direction of the interaction force F_{ik}, corresponding to the Toda or Morse potential, between the i-th and the k-th atoms in the lattice.

Let us first study analytical representations fir the case that the noise is zero. In the case of Toda interactions exists a special exact analytical solution for the square lattice by using the functions found by Toda analytically solving the 1d- equations [6–9]. The Toda solutions remain valid for the special case that the initial conditions and the corresponding excitations are strictly parallel to one axis, say the x-axis. Let n, m be the numbers denoting the nodes in x- and y-direction and let us define the compressions in x-direction by

$$\rho_{n,m}(t) = x_n(t) - x_{n+1}(t) - \sigma \tag{4}$$

Note that there are no compressions in y-direction due to the parallel dynamics inside the rows. Then with appropriate initial conditions an exact solution is given by the Toda profile running along the x-axis

$$\rho_{n,m}(t) = \frac{1}{b_T} \ln \left[1 + \frac{\sinh^2(\kappa)}{\cosh^2(\kappa n - \beta t)} \right]; \qquad \beta = \sinh(\kappa) \tag{5}$$

For small amplitudes this gives

$$\rho_{n,m}(t) \simeq \frac{1}{b_T} \frac{\sinh^2(\kappa)}{\cosh^2(\kappa n) - \beta t}. \tag{6}$$

Here b_T is the Toda stiffness, for Morse systems we find empirically a good description of the observed profile for $b \simeq b_T/3$. The constant κ is defined by the energy of the soliton. In the continuous limit this gives the well known soliton profile [6,21,22]

$$\rho(x, y, t) = \rho_0 \mathrm{sech}^2(\kappa\xi), \qquad \xi = (x \pm v_s t)/\sigma \tag{7}$$

where v_s is the soliton velocity. The soliton represented by eq.(7) is a special solution, representing a "line-soliton", of the so-called KP-equation. This equation was derived in 1970 in a pioneering paper by Kadomtsev and Petviashvili [3]. The Kadomtsev-Petviashvili equation is a kind of extension of the 1d Boussinesq- Korteweg-de Vries (BKdV) equation and reads in a standard form [3,7,9,15,16]:

$$\frac{\partial}{\partial x}\Big[\frac{\partial}{\partial t} + \frac{\partial^3}{\partial x^3}\Big]\rho(x, y, t) = \frac{\partial^2}{\partial y^2}\rho(x, y, t) + 3\frac{\partial^2}{\partial x^2}\rho^2(x, y, t) \tag{8}$$

Line solitons are extended rectilinear wave fronts localized perpendicular to the propagation direction, see also the simulations [17,18]. Let us discuss now the method of computer simulations in more detail. We solve numerically the equations of motion for the complex coordinates $Z(t)$ taking into account only those atomic units satisfying the condition $|Z_i - Z_k| < 1.5$. The dynamics of the atoms is considered to take place inside a rectangular cell $L_x \cdot L_y$ with periodic boundary conditions and depending on the symmetry of an initial distribution of units and their number $N \simeq 400$. As initial condition we assume usually a compression and velocity profile corresponding to the analytical form of a 1d Toda soliton [6–9] in a given lattice row. The other lattice units remain at their equilibrium positions on the given lattice [17,18]. As shown by Remoissenet [8], a broad spectrum of initial excitations, as e.g. excitations of rectangular profiles are able to create solitons or cnoidal waves. For this reason we have experimented with a broad range of initial conditions. For example we gave initially a suitable high momentum to one lattice site in the direction of one of the crystallographic axes in such a way that a successful start of a soliton was observed. This way we found that not only Toda profiles but also simpler initial conditions as pushing initially just one particle may be sufficient to create a soliton due to the stiffness of the exponential repulsion.

For visualization and tracking the atomic densities we modeled the atoms as little spheres with "cores" represented by a Gaussian distribution centered at each lattice site:

$$\rho(Z,t) = C \sum_{|Z - Z_i(t)| < 1.5\sigma} \exp\left[-\frac{|Z - Z_i(t)|^2}{2\lambda^2}\right]. \tag{9}$$

Using data about trajectories of particles $Z_n(t)$ and their velocities we can calculate the lattice atom distribution $\rho(Z,t)$. In Fig. 2 we show a track of the running excitation (in "bubble chamber representation") which was created by pushing just one atom in the direction of the crystallographic axis x. We show the space and time evolution of the initial soliton density peak for the time interval $\Delta t = 3$ (measured in units of $1/\omega_0$, as earlier said). The parameter values of the potential are $b\sigma = 4$, $\lambda = 0.3\sigma$. The Langevin source corresponds to a rather low temperature, $T = 0.001$ (in dimensionless units). This corresponds to the mean kinetic energy of a particle $< T_{kin} >$ reaching the value T. The soliton is moving along a crystallographic axis

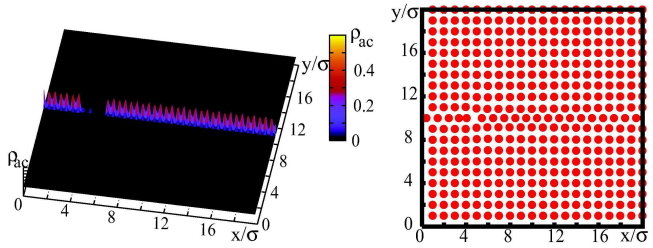

Fig. 2. Square lattice: The core density of the lattice atoms is shown in the course of time. A lattice soliton is excited by a strong pulse in $x-$ direction with velocity $2v_s$ imposed to one lattice particle located not far from the left border (site 4, row 10) along and a rather high energy $2mv_0^2$ to the 4th atom in the row. A track of the excitation (in "bubble chamber representation") of the running soliton density is represented for the time interval $\Delta t = 3$ (measured in units of $1/\omega_M$) in "bubble chamber sequence" as time proceeds. (Parameter values: $N = 400$, $b\sigma = 4$, $\lambda = 0.3\sigma$, and $T = 0.001$.)

and was excited by a strong pulse of velocity $2v_0$ imposed at $t = 0$ to the 4th atom $n = 4$ in the 10th row with rather high energy $2mv_0^2$. The high-energetic soliton excited this way is quite long lasting in its motion along the chosen crystallographic axis. Transverse excitations and thermal collisions due to the source term in the Langevin equation do not play a significant role in the interval of observation (3 time units). The phenomena studied in our simulations remind very much the discrete moving breathers observed by Marin, Eilbeck and Russell [30,31] for a wide

range of nonlinear 2-D- lattices. These authors have shown that breather excitations propagate along lattice directions at subsonic speeds and are rather robust. The results suggested broader applications including the track formation in some mica minerals and excitations in cuprates [30,31]. From the length of the cumulative path and the time interval we may estimate the velocity of the excitations demonstrated in Fig. 2. It appears that this strong local compression moves with velocity about $1.2v_{sound}$ with a lifetime of at least several time units. In the 2d triangular Morse lattice v_{sound} is slightly above 1 in our units. Solitonic excitations move a few picoseconds with nearly unaltered profile and just this robustness is the reason that we can identify them with the proposed visualization method. Losses due to scattering and radiation of linear waves are quite low, due to the nearly integrable character of the problem. Note that the 2d solitons observed here, are not line solitons but localized solitons similar to the so-called lump solutions of the KP - equations [15]. Looking at the transverse direction we find that the oscillations of the atoms in the rows adjacent to the row of maximal activity of the soliton oscillate in antiphase similar as 1d breathers [27–30]. Corresponding excitations observed in 2d-crystals were denoted as "moving breathers" [30]. We will show in the next section that the similarity to KP-solitons is so striking that we prefer to denote them as 2d-solitons [17,18].
A specific property of our solitonic excitations in square lattices is that potential energy may be released during propagation. Therefore the solitonic propagation may leave irreversible traces (see Fig. 2). The trajectories itself may be self-sustained and sometimes might be extremely long. As mentioned already, similar trajectories were observed for example as long black stripes in natural crystals of muscovite mica [29]. In theoretical work of Marin et al. [30,31] such stripes were interpreted as moving breathers. Our numerical experiments suggest that the tracks in muscovite mica could be interpreted also as high-energetic solitons generated by impacts from cosmic rays. This question has still to be discussed, we notice however that our high-energetic solitons are also very robust and may run a long path along crystallographic axes.

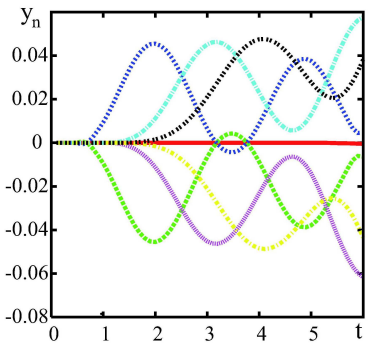

Fig. 3. Square lattice: Time evolution in the atomic rows adjacent to the (central) one in which a high energy soliton-like excitation is running (red: soliton row; dark blue and green: nearest row; light blue and pink: next-nearest row, etc. The (dimensionless) period of oscillations is below 3.

3 Dispersion relation for two-dimensional excitations and KP equation

For a linear 1d-lattice the dispersion eq for excitations in x-direction reads

$$\omega^2 = 4\sin^2(\frac{1}{2}k) \tag{10}$$

which is depicted in Fig. 4. We used here the frequency of the linear oscillations ω_0 as the unit of the frequency and the reciprocal lattice length $1/\sigma$ wave number unit. Let us search now for appropriate wave equations. Denoting the continuum limit of the strain $z_n = x_n - x_{n-1}$ as

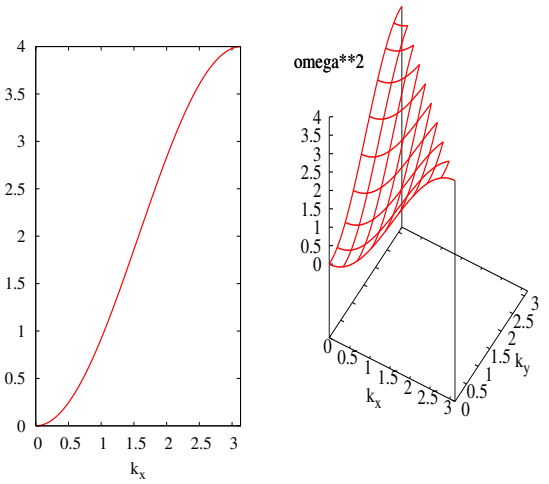

Fig. 4. The dispersion relations for 1d harmonic lattices in first Brillouin zone (left) and for 2d lattices (right panel).

the compression density $\rho(x,t)$ we arrive at a partial d.e. which was obtained already in 1877 by Boussinesq for the description of hydrodynamic waves and which belongs to the standard equations of nonlinear mathematical physics [7,9]:

$$\Big[\frac{\partial^2}{\partial t^2} - v_0^2\Big(\frac{\partial^2}{\partial x^2} + \frac{1}{12}\frac{\partial^4}{\partial x^4}\Big)\Big]\rho(x,t) = \frac{\gamma}{\kappa}\frac{\partial^2}{\partial x^2}\rho^2(x,t) \tag{11}$$

with the dispersion relation

$$\omega^2 = k^2 v_0^2\Big(1 - (k^2\sigma^2)/12 + ...\Big) \tag{12}$$

In the lowest approximation the Boussinesq equation reduces to the standard linear wave equation, which is solved by two plane waves $\rho(\xi)$ depending on the dimensionless running coordinate $\xi = (x \pm v_0 t)/\sigma$ where v_0 is the sound velocity. For the nonlinear Boussinesq equation there are two solutions for the continuous density

$$\rho(x,t) = \rho_0 \mathrm{sech}^2[\kappa\xi], \qquad \xi = (x \pm v_s t)/\sigma. \tag{13}$$

in agreement with the approximation (7) written above. The 1d solitons described by eq. (13) correspond to long wave length and hence to small wave vectors k. In the 2d-case we expect in agreement with the previous section, waves which have a similar profile in x-direction but are extended also in y-direction. Indeed there are excitations in 2d which are either line solitons or lump solitons. Both are in x-direction like the Boussinesq-Korteweg-de Vries solitons. Line solitons are extended in y- direction and lump solitons have in y-direction an envelope which is like a Gaussian.
We will show now that the KP-equation describes both phenomena. Let us consider again the case of the simplest 2d quadratic lattice A straightforward additive combination of two linear lattices would correspond to dispersion relation

$$\omega^2 = 4\sin^2(\frac{1}{2}k_x) + 4\sin^2(\frac{1}{2}k_y) \tag{14}$$

The problem with the KP-solutions, which describe observed 2d-phenomena, is that they are not symmetric along x and y. Hence eq.(14) needs some further treatment. The soliton-like

waves we have found in our computer simulations run along the x - axis like a soliton but in the direction of the y - axis the neighboring lattice units oscillate in anti-phase like breathers with amplitudes slowly decreasing along y. Because in the transverse direction the 2d-solitons behave like breathers, we should use with respect to the dispersion relation a "soliton-like" expansion along the axis x and a "breather-like" expansion into a series along the axis y. We assume that in $k_x - k_y-$ space the essential parts of the 2d-soliton dynamics appear in the region

$$|k_x| \ll 1, \qquad k_y = \pi + \Delta k_y, \qquad |\Delta k_y| \ll 1, \qquad \omega \simeq 2 \tag{15}$$

Looking at Fig. 4 the essential $k_x - k_y-$ region corresponds to the left upper corner. Accordingly we may use the expansion

$$\omega^2 = 4\left[\frac{1}{4}k_x^2 - \frac{1}{48}k_x^4\right] + 4\left[1 - \frac{1}{8}(\Delta k_y)^2\right]^2 \tag{16}$$

We introduce now a new frequency

$$\Omega = \omega^2 - 4 \tag{17}$$

and get

$$\Omega^2 - k_x^2 + \frac{1}{12}k_x^4 + (\Delta k_y)^2 = 0 \tag{18}$$

By using

$$\Omega^2 - k_x^2 = (\Omega - k_x)(\Omega + k_x) \simeq 2k_x(\Omega - k_x)$$

we arrive finally at the dispersion relation

$$2k_x(\Omega - k_x) + \frac{1}{12}k_x^4 + (\Delta k_y)^2 = 0 \tag{19}$$

corresponding to the linear weakly dispersive 2d wave equation for the compression density

$$\frac{\partial}{\partial x}\Big[\frac{\partial}{\partial t} + v_0\frac{\partial}{\partial x} + \frac{v_0\sigma^2}{24}\frac{\partial^3}{\partial x^3}\Big]\rho(x,y,t) = \frac{v_0}{2}\frac{\partial^2}{\partial y^2}\rho(x,y,t) \tag{20}$$

This is nothing else than a linear version of the KP- equation. By comparing our weakly dispersive 2d wave equation (20) with the KP-equation (8) we see that a nonlinear term on the r.h.s is missing. By adding this term which is known to us already from the Boussinesq equation we find the KP-equation in physical variables as used e.g. for the description of shallow water waves [16]:

$$\frac{\partial}{\partial x}\Big[\frac{\partial}{\partial t} + v_0\frac{\partial}{\partial x} + \frac{v_0\sigma^2}{24}\frac{\partial^3}{\partial x^3}\Big]\rho(x,y,t) = \frac{v_0}{2}\frac{\partial^2}{\partial y^2}\rho(x,y,t) - v_0\gamma\frac{\partial^2}{\partial x^2}\rho^2(x,y,t) \tag{21}$$

This equation is also exactly solvable as found by Zakharov and Shabat [4] and others [15,16]. However the structure of the manifold of solutions is much richer than that of the BKdV equation [16]. There exist line solutions which are localized along certain lines in two-dimensional planes. These solutions are plane waves which in simplest case are generalizations of the BKdV-solitons [15]. There exist many other line solutions [16]. A second class of solutions represent the so-called lump solitons which are like moving hills. A special solution for the envelope of a lump-type soliton reads [7,15]:

$$\rho(x,y,t) = \rho_0\frac{[v_s y^2 + 3/v_s - (x - v_s t)^2]}{[v_s y^2 + 3/v_s + (x - v_s t)^2]^2} \tag{22}$$

Note that this special solution depends only on one parameter v_s which is the soliton velocity and has positive and negative parts. This is related to the property that the integral is zero

$$\int dxdy\rho(x,y,t) = 0; \rho_0 = \frac{v_s}{3}. \tag{23}$$

In Fig. 5 we represented the envelope of a lump soliton at two subsequent time instants. Such lump solutions we have found numerically for Morse lattices in section 2 and in [17,18].

We come to the conclusion that the the type of solitons found in our simulations for Morse lattices corresponds with respect to the envelope to the type of lump solitons.

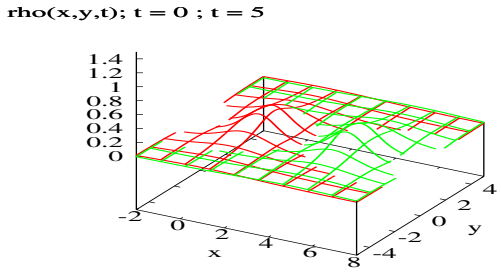

Fig. 5. Solution of the KP equation showing a travelling lump soliton at two successive time instants.

4 Stabilization of square lattice by onsite interactions - CuO_2 lattices

Heating square lattices with Morse interactions shows that this lattice configuration is thermally unstable. We have demonstrated this by simulations with increasing strength of the noise source in the Langevin equations (3). An illustration of the thermal instability is depicted in Fig. 6. We heated an initially square lattice in contact with a heat bath of temperature $T = 0.1$ up to the time $t = 5$. Then we switched the heat bath off and made a snapshot after time $t = 50$. What we observe is the occurrence of local defects and local transitions to the more stable triangular lattice. This shows that the square lattice is globally unstable. Before we study the

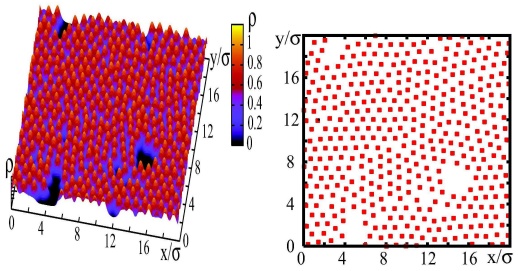

Fig. 6. Square lattice of heated Morse atoms: by heating of an initially square lattice occure more and more defects. We show the landscape of the deformation density (left panel) and the distorted lattice structure (right panel). Parameter values: $N = 400, b\sigma = 4, T = 0.1, t = 50$.

more stable triangular structures, let us investigate a method of stabilization by fixed onsite interactions. We introduce interactions with a second square lattice with motionless units fixed in space. Such modified square configurations are very stable and are observed in nature e.g. in the CuO_2-layers of the Cuprates [31,32] Fig. 7 shows a stable configuration of an Oxygen lattice imbedded into a rigid motionless copper lattice. The parameters of the assumed Morse interactions were adapted in the following way. The relation of the radii was obtained from the geometrical argument, that the relation $1/\sqrt{2}$ is optimal. Further we took qualitatively into account that the the bonds $Cu - O$ are stronger than the bonds $O - O$. Therefore we used in our model:

$$\frac{\sigma_{CuO}}{\sigma_{OO}} = 1/\sqrt{2}; \qquad \frac{D_{CuO}}{D_{OO}} = 2$$

This way we obtained a stable lattice consisting of two square lattices depicted in Fig. 7. This stable $Cu - O-$ lattice is not able to bear solitons due to the big distances between the

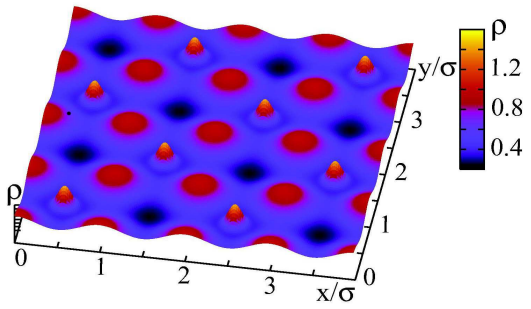

Fig. 7. Two square lattices: The unstable square lattice of Oxygen is in copper oxide stabilized by a second fixed square lattice of Cu-atoms (the narrow peaks in our picture). Parameter values: $(b\sigma)_{OO} = 7, (b\sigma)_{CuO} = 10, D_{CuO} = 2D_{OO} = 2, \sigma_{CuO} = 0.707\sigma_{OO}$.

movable elements, the oxygen atoms as to be seen in Fig. 7. We have just to remember that the generation of solitons requires that the atoms come near to each other and feel strong repulsive forces. What we need for bearing solitonic excitations, are rectilinear rows of strongly repulsive atoms with small distances in the range of repulsive forces.
Several authors claim that solitons and bisolitons play a leading role for the explanation of the superconduction of the cuprates [32]. How such solitons or bisolitons could arise in spite of the unfavorable conditions in normal $Cu-O-$ lattices? We have shown in recent work that with electron or hole doping, the conditions for the generation of solitons are favorable. This is due to the fact that doping induces a change of the bond length. As a consequence the $Cu-O-$ lattice may be rearranges creating stripes of atoms $O-O-O-O-...$ which might be streets for the propagation of solitons. In order to study this effect we assumed that electrons or holes introduced by doping may increase he relations between the radii of Cu and O. For illustration we assumed a different geometrical relation for the bond length and also some larger relation for the bond strength

$$\frac{\sigma_{CuO}}{\sigma_{OO}} = \frac{\sqrt{3}}{2}; \qquad \frac{D_{CuO}}{D_{OO}} = 4$$

Our computer simulations show, as depicted in Fig. 8 that changing bond length may generate crystal structures with rectilinear rows of Oxygen. Possibly these stripes of Oxygen atoms, might be good streets for the propagation od solitons in cuprates. It might be interesting to note that the formation of stripes in Cuprates is a well known phenomenon [33]. This observation might support our assumptions.

In the next section we turn to the much simpler case of triangular lattices which are very stable and contain from the very beginning atomic rows able to propagate solitons [17,18].

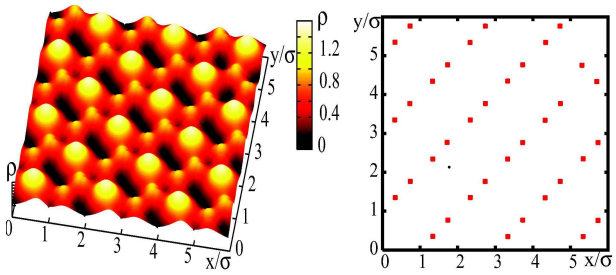

Fig. 8. By changing the bond length, possibly through doping, we may generate stable lattices which are able to carry solitons. Parameters: $(b\sigma)_{OO} = 5, (b\sigma)_{CuO} = 10, D_{CuO} = 4D_{OO}, \sigma_{CuO} = 0.87\sigma_{OO}$.

5 Excitations in triangular lattices and interactions with charges

In the triangular lattice, which is the simplest stable lattice, it is not difficult to generate solitons by appropriate initial conditions [17,18]. We were able to generate line solitons of finite length and studied their behavior at collisions. Further by exciting atoms in one row along a crystallographic axis we could generate lump solitons running along that crystallographic axis. The Hamiltonian we used for the simulations is just the same as in Section 2 with the difference that the initial conditions correspond to an equilibrium triangular lattice now. We simulated initially $N = 400$ particles with periodic boundary conditions, the parameters of the Morse interactions were $b\sigma = 4$. In Fig. 9 we show an example of a lump soliton which was excited by a strong kick. Starting with a lattice at rest we attributed an initial velocity $v_0 = 2$ to just one atom located at $x = 4, y = 9$ in direction of the x-axis. The corresponding momentum is transmitted to the next neighbor at right etc.. and this way a solitonic excitation is created.

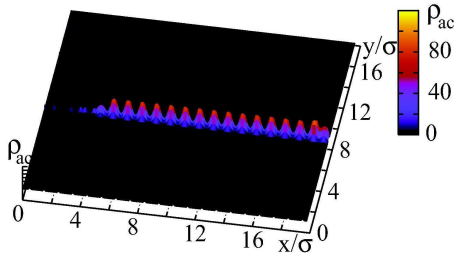

Fig. 9. Triangular lattice: The moving soliton-like compression density along a crystallographic axis in a triangular lattice without electrons ($N = 400$, $b\sigma = 4$). The excitation moves with supersonic velocity.

Following earlier work [25,26] we will show now that lump solitons are able to carry electrons (or holes) surfing on the compression wave. We consider a system consisting of atoms arranged initially on a triangular lattice and additional electrons moving from site to site and interacting with the atoms. In order to study the evolution of the quantum states of the additional electrons interacting with the atoms in the 2d-lattice, we assume a standard tight-binding description. Let n, m denote the internal quantum numbers of the states of electrons bound to the corresponding atoms at sites $\mathbf{r}_n$ and $\mathbf{r}_m$. In the following we will assume for simplicity, that there is only one quantum state per atom which can be occupied by the external electrons. If necessary, the internal state that characterizes the orbit as well as spin, can be included in the quantum number n. We set the electronic Hamiltonian

$$H_e = \sum_n E_n c_n^+ c_n + \sum_{n,n'} t_{n,n'} c_{n'}^+ c_n \,. \tag{24}$$

The energy levels E_n will be approximated by constant values $E_n = E_0$. The transition matrix elements $t_{n,n'}$ depend in our model on the atomic distances, $t_{n,n'} = t(\mathbf{r}_{n'} - \mathbf{r}_n)$. Following Slater and others we take an exponential dependence

$$t_{n,n'} = V_0 \exp[-\alpha_h |\mathbf{r}_n - \mathbf{r}_{n'}|] \,. \tag{25}$$

The range parameter α_h can be related to the tunneling probability that decreases exponentially with distance.
For the lattice part, the Hamiltonian with Morse interactions reads as above. As before the characteristic length determining the repulsion between the particles in the lattice is σ. We limit ourselves to nearest-neighbors only using the relative distance with $r_{kj} = |\mathbf{r}_k - \mathbf{r}_j|$. Also as before by imposing the cutoff of the potential at 1.5σ, we exclude unphysical cumulative interaction effects arising from the influence of lattice units outside the first neighborhood of each

atom [25]. Introducing complex coordinates $Z_n = x_n - iy_n$ we write the discrete Schrödinger equation for the electrons and the Newton equations for the atoms in the form ($\tau = V_0/\hbar\omega_0$):

$$\frac{dc_n}{dt} = i\tau \exp(\alpha b\sigma) \sum_{m\neq n, |Z_n - Z_m|<1.5} c_m \exp(-\alpha|Z_n - Z_m|) \tag{26}$$

$$\frac{d^2 Z_n}{dt^2} = \sum_{m\neq n, |Z_n - Z_m|<1.5} [\exp(b\sigma - |Z_n - Z_m|)$$
$$(1 - \exp(b\sigma - |Z_n - Z_m|)) + 2\alpha V_0 \exp(\alpha b\sigma - |Z_n - Z_m|) Re(c_n c_m^*)] \frac{Z_n - Z_m}{|Z_n - Z_m|} \tag{27}$$

For the simulations we use again dimensionless units, i.e. lengths are measured in units σ, times in units of the reciprocal frequency around the minimum of the atomic interaction potential $1/\omega_0$. For purpose of a better visualization we replace all points resulting from the simulations by little Gaussian balls representing the wave functions at the corresponding site. In a first run we look at the dynamics of electrons decoupled from the lattice (see Fig. 10). We observe the typical spreading of the free wave functions. In a second run we switch on the interaction

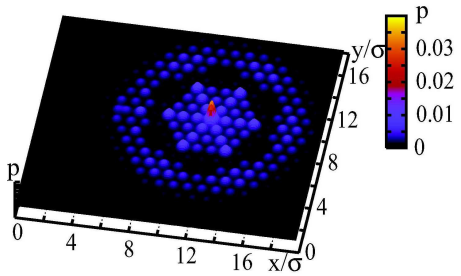

Fig. 10. Triangular lattice: Spreading of the smoothed density distribution of a free electron at $t = 0.2$ which was inserted at $t = 0$ at just one lattice point. Besides the typical spreading of the wave function, we see some structuring which is due to the lattice symmetry with 3 crystallographic axes and to the periodic b.c. ($N = 400, b\sigma = 4, \tau = 10, \alpha = 0$).

with the lattice on which a soliton is running. Surprisingly enough the electron density is all gathered by the soliton and both move together, the electron is surfing on the soliton (see Fig. 11).

The simulations are carried out by solving numerically the set of equations given above for 400 atoms and 1 electron. We are well aware that simulations for a matrix of 20 to 20 sites still need a careful check for finite size effects. Preliminary tests with 1600 particles (in part presented in the next section) have however shown that the basic effect demonstrated here, the formation of moving bound states between lattice excitations and electrons is only weakly size dependent. We note that similar phenomena of collecting electron density by solitons in 2d-lattices were recently observed also by Cisneros-Ake and Minzoni [38]. There seems to be also some analogy to recent experiments about controlling electrons by strong surface acoustic waves [23,24]. However a direct comparison of our simulations for small lattices with the experiments on the millimeter - scale [23,24] is not possible. We may assume, however that the basic effects of coupling electron-lattice excitations remain the same or are at least similar.

6 Lossfree charge transport

The numerical experiments described in the preceding section illustrate a new way of of charge transfer from a point A in a 2d-layer to a point B as far as both points are located along

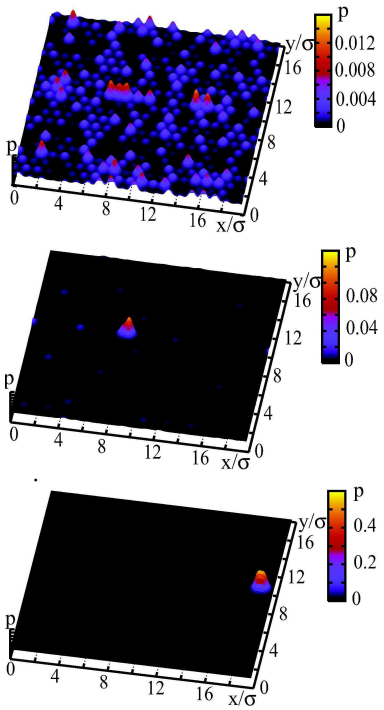

Fig. 11. Triangular lattice: Including the interaction with the lattice ($\alpha = 0.5, V_0 = 1$), on which like in Fig. 9 a soliton is running, the electron feels the compressions created by the soliton and starts to concentrate around the compression density. With increasing time (above $t = 0.8$, center $t = 1.0$, below $t = 6.0$) the electron density is more and more concentrated around the compression density and moves finally with the soliton with supersonic velocity along the crystallographic axis .

a crystallographic axis. As shown in Fig. 11, the soliton is able through the formation of a solectron bound state to carry an electron nearly free of losses at least on a distance of 20 crystallographic units, i.e. possibly around $10nm$ in a time interval of $t \simeq 6$ in units of the oscillation time. Over this relatively short time and short distance no damping is seen, i.e. the transfer is nearly loss-free. We see, that the 2d-solectron propagating along a crystallographic axis which is the carrier of the observed effect is a nearly conservative process. This is connected with several circumstances:
(i) In the longitudinal direction i.e. along the axis of propagation, the soliton is a 1d- ballistic excitation for which energy is conserved.
(ii) In perpendicular direction, i.e. across the crystallographic axis of propagation, the excitations are breather-like, i.e. they are in a window of non-transparency and cannot propagate. This is related to the dispersion relations discussed in section 3.
Of course, some losses cannot be avoided, however the losses are for this kind of charge transfer very weak in comparison with standard ways of charge transfer which are connected with the emission of phonons preferentially in perpendicular direction. In our case, the phonon emission is weak due to fact that in the operating regime, phonons are in the window of non-transparency. In order to study the life time of solectronic excitations in more detail, we studied a sample with a rather long channel-like two-dimensional crystal containing $N = 20 \cdot 80 = 1600$ particles. Looking at Fig. 12 we see
(i) the transversal extension similar as predicted by the solution of the KP equation (22),
(ii) the absence of significant losses leading to a nearly ballistic propagation.
The directed motion of an electron guided by a soliton along crystallographic axis carries a current. Adapting the quantum-mechanical formula to a linear lattice we calculated the mean

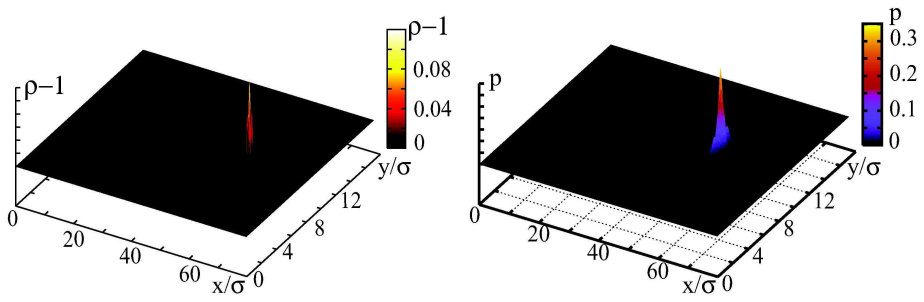

Fig. 12. Triangular lattice: Soliton compression density (panel above) and corresponding solectron probability density (panel below) density in a channel-like lattice of $N = 20 \cdot 80 = 1600$ particles. ($b\sigma = 4$). The soliton was created by attributing in a lattice at rest the velocity $v_0 = 2$ in $x-$ direction to the atom at $x = 10, y = 9$. We see that the compression density (above) and the charge probability density (below) coincide very well even after a relatively long time of propagation $t = 50$.

current from [36,37]

$$j = i \sum_n [c_n(c^*_{n+1} - c^*_n) - c^*_n(c_{n+1} - c_n)] = i \sum_n [c^*_{n+1}c_n - c^*_n c_{n+1}] \tag{28}$$

In application of formula to the current along a crystallographic axis, the elements have to be numbered accordingly. The results show a strongly fluctuating in time and slowly decaying current, see Fig. 13. We observe a rather weak decay of the current with a long tail, the decay time is around 50 - 100 in our time units given by $1/\omega_0$. The decay to zero may be overtaken by an electric field. In order to study the effect of an electric field we may add a corresponding term

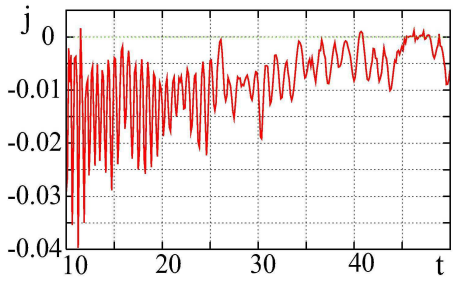

Fig. 13. Long time evolution and slow decay of the electric current generated by the soliton shown in Fig. 1212 in the time interval $10 < t < 50$ ($N = 1600$).

to the TBA equations as in [36,37]. We shall deal with this problem elsewhere. The current obtained in our simulations is strongly fluctuating in time and is nearly loss-free. The value of the electron current (the drift velocity) is determined mainly by the soliton velocity. We note that similar electron currents were observed experimentally by Donovan and Wilson on samples of PDA- and PDTA-crystals [39–41].

7 Discussion

We studied the dynamics of soliton-like excitations in several two-dimensional lattices: square lattice, square lattice with onsite stabilization, and triangular lattice including interaction with charges.

In the first part we studied beside simulations, dispersion laws of 2d solitons and basic solutions of the Kadomtsev-Petiashvili theory in comparison to our simulations. Further we have developed theoretical tools for the study of *slaved* individual electron evolution by means of lattice soliton-like excitations acting as carriers along the crystallographic axes of a e.g. a triangular lattice. We have shown that for each crystallographic axis there exist stable electron-soliton bound states, called solectrons. The velocity of solectrons may be higher than $1000m/s$ in a solid medium, faster than the drift velocities of "free" electrons, which usually do not exceed $1 - 100cm/s$. Such high electron velocities were observed experimentally in crystals of PDA and PDTA by Donovan and Wilson [39–41]. Therefore there is not only theoretical but also experimental evidence that solitonic excitations may create bound states which are able to carry electrons at near-to-sound velocity over a distance of a few hundred sites. We have shown that there is no significant loss of electron energy and momentum. This appears as a clear case of electron surfing. Our most interesting result is, that due to the conservative character of soliton motion and the fast decay of lump solitons in transversal directions, the electron transfer is nearly lossfree. By means of external electric fields, a fast current with electron velocities around the sound velocity may be obtained.

The authors are grateful to Vadim S. Anishchenko for decades of friendship and collaboration; W.E. and M.G.V. have also to thank for warm hospitality at State University of Saratov. Further the authors acknowledge fruitful discussions and correspondence with L. Cruzeiro, D. Hennig, G. Röpke and F.M. Russell. L.A. Cisneros-Ake is also gratefully acknowledged for giving in December 2012 at a research meeting at UCM a talk on recent results for a 2D Davydov-Scott anharmonic model. The authors also wish to thank V.I. Nayanov, C. Ford, A. Wixforth, R.P.G. McNeil, T. Meunier for sharing with us their nonlinear acoustic wave and electron surfing experiments in piezoelectric layers. E.G. Wilson is also gratefully acknowledged for detailed information on his experiments on soliton-mediated charge motion in PDA crystals.

This research was supported by the Spanish Ministerio de Ciencia e Innovacion, under Grant MAT2011-26221 and by the Ministry of Education and Science of the Russian Federation within FTP Scientific and pedagogical personnel of the innovative Russia, 2009-2013, grant 14.B37.21.0751.

References

1. V.S. Anishchenko, V.V. Astakhov, A.B. Neiman, T.E. Vadivasova, L. Schimansky-Geier, *Nonlinear dynamics of chaotic and stochastic systems*, 2nd edn., Springer-Verlag, New York, 2002.
2. V. S. Anishchenko, O. V. Sosnovtseva, A. S. Kopejkin, D. D. Matujshkin, A. V. Klimshin, Synchronization effects in networks of stochastic bistable oscillators, Mathematics and Computers in Simulation **58**, 469 - 476, 2002.
3. B.B. Kadomtsev, V.I. Petiashvili, On the stability of solitary waves in weakly dispersive media, Soviet Phys. Doklady **15**: 539-41, 1970.
4. V.E. Zakharov, A.B. Shabat, A scheme for integrating the nonlinear equations of mathematical physics by the method of the inverse scattering problem, Funct. Anal. Appl. **8**, 226-235, 1974.
5. V.S. Manakov, V.E. Zakharov, L.A. Bordag, V.B. Matveev, Two-dimensional solitons of the Kadomtsev-Petviashvili equation and their interaction, Phys. Lett. A **63**, 205-206, 1977.
6. M. Toda, *Theory of nonlinear lattices*, 2nd edn., Springer-Verlag, New York, 1989.
7. M.I. Ablowitz, P. Clarkson, Solitons, nonlinear evolutions and inverse scattering, Cambridge University Press, 1992.
8. M. Remoissenet, *Waves Called Solitons. Concepts and Experiments*, Springer, Berlin 2010.
9. N.A. Kudryashov, Methods of nonlinear mathematical physics (in Russ.), Publ. Intellekt, Dolgoprudnyi 2010.
10. C.I. Christov, M.G. Velarde, Int. J. Bifurcation & Chaos **4**, 1095, 1994.
11. A.A. Nepomnyashchy, M.G. Velarde, Phys. Fluids **6**: 187 - 189, 1994.
12. A.A. Nepomnyashchy, M.G. Velarde, P. Colinet, *Interfacial Phenomena and Convection*, Chapman & Hall/CRC, London, 2002.
13. C.I. Christov, G.A. Maugin, M.G. Velarde, Phys. Rev. E **54**, 3621, 1996.
14. H. Linde, M.G. Velarde, W. Waldhelm, A. Wierschem, J. Colloid & Interface Science **236**, 214 -224, 2001.

15. A.A. Minzoni, N.F. Smyth, Evolution of lump solutions for the KP equation, Wave Motion **24**, 291 - 305, 1996.
16. Y. Kodama, KP solutions in shallow water, J. Phys. A: Math. Theor. **43**, 43004, 2010.
17. A.P. Chetverikov, W. Ebeling, M.G. Velarde, Properties of nano-scale soliton-like excitations in two-dimensional lattice layers. Physica D **240**, 1954–1959, 2011.
18. A.P. Chetverikov, W. Ebeling, M.G. Velarde, Localized nonlinear, soliton-like waves in two-dimensional anharmonic lattices. Wave Motion **48**, 753–760, 2011.
19. V.I. Nayanov, JETP Phys. Lett. **44**, 314–316, 1986.
20. C. Rocke et al., Phys. Rev. Lett. **78**, 4099, 1997; M. Rotter et al., Phys. Rev. Lett. **82**, 2171, 1999; M. Streibl et al., Appl. Phys. Lett. **75**, 4139, 1999.
21. A.S. Davydov, *Solitons in Molecular Systems*, 2nd edn. Reidel, Dordrecht, 1991.
22. A.V. Zolotaryuk, K.H. Spatschek, A.V. Savin, Supersonic mechanism for charge and energy transfers in anharmonic molecular chains, Phys. Rev. B **54**, 266–277, 1996.
23. S. Hermelin, S. Takada, M. Yamamoto, S. Tarucha, A.D. Wieck, L. Saminadayar, C. Bäuerle, T. Meunier, Nature **477**, 435–438, 2011.
24. R.P.G. McNeil, M. Kataoka, C.J.B. Ford, C.H.W. Barnes, D. Anderson, G.A.C. Jones, I. Farrer, D.A. Ritchie, Nature **477**, 439–442, 2011.
25. A.P. Chetverikov, W. Ebeling, M.G. Velarde, Eur. Phys. J. B **70**, 117 (2009); **80**, 137–145 (2011)
26. A.P. Chetverikov, W. Ebeling, G. Röpke, M.G. Velarde, Contr. Plasma Phys. **51**, 814–829 (2011)
27. S. Aubry, Breathers in nonlinear lattices: existence, linear stability and quantization, Physica D, **103**, 201-250, 1997.
28. S. Flach, A.V. Gorbach, Discrete Breathers. Advances in Theory and Applications. Physics Reports **467**, 1-116, 2008.
29. Christiansen, P.L.; Sorensen, M.P.; Scott, A.C. (Eds.): Nonlinear Science at the Dawn of the 21st Century, Lecture Notes in Physics, Vol. 542, Springer, Berlin 1999.
30. J.L. Marin, J.C. Eilbeck, F.M. Russell, Phys. Lett. **248**, 225, 1998; **A 281**, 21, 2001.
31. F.M. Russell, J.C. Eilbeck, Eur. Phys. Lett. **78**, 1004, 2007.
32. A. Mourachkine, High-temperature superconductivity in cuprates, Kluwer, Dordrecht 2002
33. K.A. Moler, High-temperature superconductivity: How the cuprates hid their stripes. Nature 468, 643-644, 2010.
34. M.G. Velarde, W. Ebeling, A.P. Chetverikov, Soliton-mediated compression density waves and charge density in 2d layers of underdoped cuprate-like lattices. Comtes Rendus Mecanique **340**, 910-916, 2012.
35. M.G. Velarde W. Ebeling, A. P. Chetverikov, Localized excitations and anisotropic directional ordering in a two-dimensional Morse lattice model of cuprate layers, Proceedings LENCOS-2012 (to appear).
36. D. Hennig, A. Neissner, M.G. Velarde, W. Ebeling, Effect of anharmonicity on charge transport in hydrogen-bonded systems, Phys. Rev. E **76**, 046602, 2007.
37. M.G. Velarde, W. Ebeling, A.P. Chetverikov, D. Hennig, Electron trapping by solitons. Classical versus quantum mechanical approach. Int. J. Bifurcation Chaos **18**, 521–526 (2008)
38. L. A. Cisneros-Ake, A.A. Minzoni, Solectron propagation in a 2D Davydov-Scott anharmonic model, Seminar at a Research Meeting, UCM Madrid, December 2012.
39. K.J. Donovan, E.G. Wilson, Phil. Mag. B **44**, 9–29, 31 – 45 (1981)
40. E.G. Wilson, J. Phys. C, Sol. Stat. Phys. **16**, 6739–6755 (1983)
41. K.J. Donovan, P.D. Freeman, E.G. Wilson, J. Phys. C **18**, L275–L282 (1985)